

Superconductivity in $\text{Bi}_2\text{Sr}_2\text{CaCu}_2\text{O}_{8+\delta}$ single crystals doped with Fe, Ni, and Zn

B. vom Hedt, W. Lisseck, K. Westerholt, and H. Bach

Institut für Experimentalphysik IV, Ruhr-Universität, D-44780 Bochum, Germany

(Received 15 November 1993)

We report electrical conductivity and magnetization measurements on single crystals of the high- T_c superconductor $\text{Bi}_2\text{Sr}_2\text{CaCu}_2\text{O}_{8+\delta}$ with partial substitution of Fe, Ni, and Zn for Cu. Even concentrations of the doping element below 1 at. % cause a strong increase of the electrical resistivity, a definite increase of the London penetration depth, and a decrease of the correlation length. Concomitantly the critical current is lowered and the irreversibility line shifts towards lower field values with increasing concentration of the dopants. For the initial slope dT_c/dx we derive a value of -5 K/at. % independent of the substitutional element.

I. INTRODUCTION

The method of systematic creation of point defects in the CuO_2 planes of the high-temperature superconductors by replacing the Cu atoms by other $3d$ elements is a useful tool for probing parameters essential for the superconductivity. The change of the normal electronic conductivity when point defects are introduced into the CuO_2 planes, for example, can give information about the interaction of the charge carriers with the impurity. There is experimental evidence that impurities in the CuO_2 planes, even if they are nonmagnetic, can change the magnetism of the neighboring Cu spins drastically by inducing local Cu moments, or, in the holon-spinon language, by causing the condensation of a spinon.¹⁻³

The superconductivity of the high- T_c cuprates is generally strongly suppressed by substitutional elements in the CuO_2 planes. In the system $(\text{La}_{1-x}\text{Sr}_x)_2\text{CuO}_4$, about 4 at. % of substitution in the Cu position is sufficient to quench the superconductivity.^{4,5} In n -type superconductors like $(\text{Pr}_{1-x}\text{Ce}_x)_2\text{CuO}_4$, the influence is even stronger, and Ni and Fe concentrations below 1 at. % suppress the superconductivity completely.^{6,7}

The majority of papers published on high- T_c compounds with substitution for Cu deal with the system $\text{YBa}_2\text{Cu}_3\text{O}_{7-\delta}$ (see Refs. 8–10 and references therein). In this system, nonmagnetic Zn is especially effective in suppressing T_c . However, in $\text{YBa}_2\text{Cu}_3\text{O}_{7-\delta}$ the situation is more complex than in the $\text{La}(1:2:4)$ system, since two different positions, the chain Cu(1) position and the plane Cu(2) position, exist in the unit cell and a dopant can substitute for Cu at Cu(1) or Cu(2). The influence of substitution in the chain and plane positions on the superconductivity is very different. Substitution in the chain mainly acts indirectly via modification of the intercell charge transfer and thus the number of holes in the CuO_2 planes.¹¹ Dopants in the CuO_2 planes suppress the superconductivity directly, as in the $\text{La}(1:2:4)$ compounds. Detailed neutron and x-ray work has been devoted to the problem of the site preference for a specific substituent at Cu(1) or Cu(2),^{12,13} and one finds roughly that 3^+ ions mainly substitute in the chains and 2^+ ions both in the

plane and the chain, but especially at low concentration the site preference is still somewhat controversial.

The origin of the suppression of T_c by point defects in the CuO_2 planes is not yet very clear. One important mechanism of the suppression of T_c might be the disorder introduced by the substitutional elements. Since the superconductors are quasi-two-dimensional, scattering of the charge carriers by disorder can decrease T_c .^{14,15}

Comparing with conventional superconductors, one would expect that pair-breaking scattering on impurity spins should be very effective in suppressing T_c . A puzzling result for p -type high- T_c compounds, however, is that the conventional Abrikosov-Gorkov type of spin scattering on the impurity spins is not effective. In $(\text{La}_{1-x}\text{Sr}_x)_2\text{CuO}_4$, T_c is suppressed at the same rate for magnetic and nonmagnetic substituents,^{4,5} and in $\text{YBa}_2\text{Cu}_3\text{O}_{7-\delta}$ the substitution of Zn is more effective in suppressing T_c than Ni or Fe.⁸⁻¹⁰

There are, however, clear indications from experiments that a pair-breaking process is nevertheless active in the doped p -type high- T_c superconductors. One has observed a strong suppression of the specific-heat peak¹⁶ and a rapid narrowing of the superconducting gap with doping,^{17,18} strongly reminiscent of what is expected for a pair-breaking scattering process in conventional superconductors.

Candidates for the pair-breaking scattering process are an indirect magnetic Abrikosov-Gorkov process on the magnetic Cu moments induced by the dopants^{2,3} or a nonmagnetic scattering process, if the symmetry of the order parameter is not of s type.¹⁹ In the latter case, the Anderson theorem does not hold and nonmagnetic elastic scattering can be pair breaking.

The subject of the present paper is a study on single crystals of the $\text{Bi}(2:2:1:2)$ system with substitution of Fe, Ni, and Zn in the Cu position. Only a few publications on polycrystalline $\text{Bi}(2:2:1:2)$ with different doping elements exist in the literature until now.²⁰⁻²² We know of only one paper on single crystals of $\text{Bi}(2:2:1:2)$ with doping of Co.¹⁸

The superconducting $\text{Bi}(2:2:1:2)$ phase is well suited for a study of the influence of doping elements in the CuO_2 planes, since there is only one position of Cu in the unit

cell and the growing of homogeneous single-phase crystals is possible. Measurements on single crystals give more reliable quantitative information than measurements on polycrystalline material. For example, the formation of impurity phases in grain boundaries enriched in the doping element can severely affect the shift of T_c with doping in polycrystalline material. A quantitative analysis of the anisotropic resistivity, magnetoresistivity, or reversible susceptibility in order to derive microscopic parameters is also impossible in polycrystalline material, but strongly desirable for a deeper insight into the effects caused by an impurity in the CuO_2 planes.

II. PREPARATION AND EXPERIMENTAL

Single crystals of the high-temperature superconducting phase $\text{Bi}_2\text{Sr}_2\text{CaCu}_2\text{O}_{8+\delta}$ with partial substitution of Fe, Ni, and Zn for Cu were grown by a modified Bridgman-Stockbarger technique. Stoichiometric portions of Bi_2O_3 , SrCO_3 , CaCO_3 , CuO , and Fe_2O_3 , NiO , ZnO were mixed thoroughly, decarbonized at 800°C in air, and melted in an Al_2O_3 crucible. The crucible was then lowered slowly in the temperature gradient of a rf-induction furnace in order to allow for directional solidification (for details see Ref. 23). The crystals were separated mechanically from the solidified ingot. They possessed a distinct cleavage plane perpendicular to the c axis and had a dimension up to $3 \times 2 \times 0.1 \text{ mm}^3$. Before the measurements the crystals were homogenized by annealing at 800°C in an atmosphere of 8% O_2 and 92% Ar.

The composition of the crystals was determined quantitatively by x-ray wavelength-dispersive microprobe analysis. The concentration of the doping elements in the crystals was found to be homogeneous but deviated strongly from the nominal composition in the melt and scattered slightly even for crystals from the same ingot. We therefore have determined the concentration of the dopant for each crystal of the present study separately. The effective substitution coefficient for the Fe-, Ni-, and Zn-doped crystals is shown in Fig. 1 where we have plotted the true dopant concentration in the crystals versus the nominal concentration in the melt. The true Zn concentration levels off already at a concentration of 0.4 at.%; thus we could not get crystals containing more than 0.4 at. % of Zn. The same limit for Ni is about 2 at. %. We find that Fe is enriched in the crystals compared to the melt and we got crystals with up to 9 at. % of Fe. The crystal size, however, was found to decrease strongly for higher Fe concentrations.

The lattice parameters of the crystals were determined by x-ray Bragg reflection patterns and are summarized in Figs. 2(a)–2(c). The samples crystallize in the orthorhombic space group Amma .²⁴ The c -axis length decreases with increasing Ni concentration and increases with the Fe concentration, consistent with the published data on polycrystalline doped $\text{Bi}(2:2:1:2)$ samples.^{18,20–22} We note that we did not find a shrinking of the unit-cell volume as reported for Co-doped $\text{Bi}(2:2:1:2)$ single crystals in Ref. 18 and attributed there to nonstoichiometry developing with the doping.

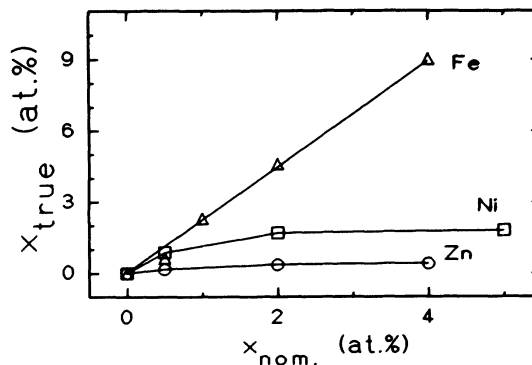


FIG. 1. True dopant concentration of the $\text{Bi}_2\text{Sr}_2\text{Ca}(\text{Cu}_{1-x}\text{M}_x)_2\text{O}_{8+\delta}$ crystals versus the nominal dopant concentration in the melt.

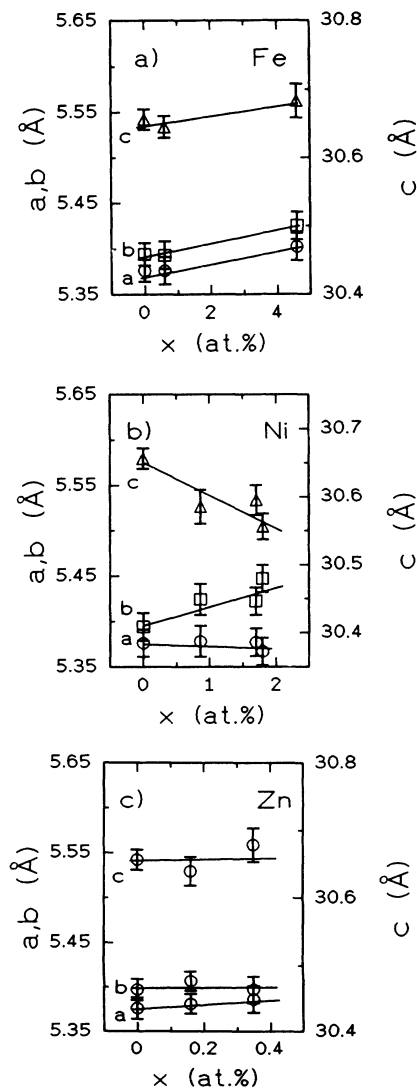


FIG. 2. (a)–(c) Lattice parameters of the Fe-, Ni-, and Zn-doped $\text{Bi}(2:2:1:2)$ crystals versus the impurity concentration.

For the dc-magnetization measurements at low fields we used a noncommercial superconducting quantum interference device (SQUID) magnetometer described in detail in Ref. 25. For the magnetic-hysteresis measurements at high fields we used a vibrating-sample magnetometer with a superconducting solenoid for fields up to 10 T.

The electrical-resistivity measurements were done by the four-point low-frequency ac technique. The electrical contacts were made by silver paint heated to 300°C to achieve good Ohmic contacts with a contact resistance of typically 1 Ω . The current contacts covered the whole (100) face of the crystals in order to ensure good homogeneity of the current. For several crystals the resistance was determined by the Montgomery technique in addition; the overall agreement of the absolute values of ρ_{ab} between these two methods was found to be good.

For the magnetoresistance measurements we used a superconducting split-coil assembly with a horizontal magnetic field up to 5 T. The samples could be adjusted by rotation perpendicular to the magnetic-field axis with a precision of 1°.

III. RESULTS AND DISCUSSION

In Fig. 3 we show the zero-field-cooled magnetic-susceptibility curves measured in a low field of 5 Oe perpendicular to the CuO_2 planes for a single crystal of the pure $\text{Bi}(2:2:1:2)$ phase and for the doped crystals. The transition shifts continuously towards lower temperatures with increasing dopant concentration and remains sharp up to a concentration of the dopant of about 2 at. %. For the Fe-doped samples with concentrations above 2 at. % the transition is strongly broadened, indicating an inhomogeneous distribution and clustering of the Fe atoms.

In Fig. 4 we plot the transition temperatures defined by

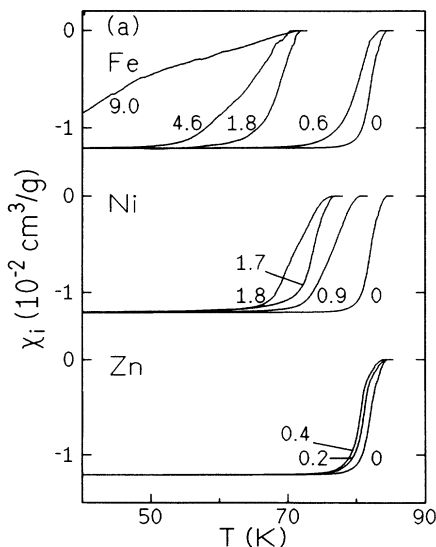


FIG. 3. Zero-field-cooled magnetic susceptibility versus temperature measured at 5 Oe for $\text{Bi}(2:2:1:2)$ single crystals with Fe, Ni, and Zn. The numbers in the figure give the dopant concentration in at. % of Cu. The data have been corrected for the demagnetizing field.

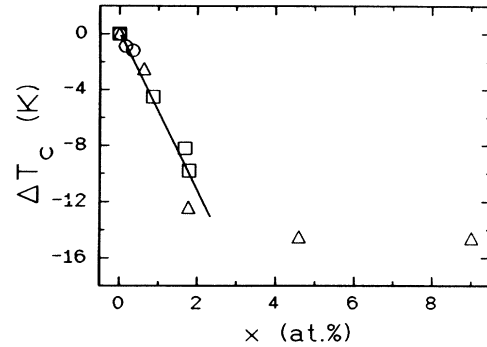


FIG. 4. Superconducting transition temperature versus dopant concentration for $\text{Bi}_2\text{Sr}_2\text{Ca}(\text{Cu}_{1-x}\text{M}_x)_2\text{O}_{8+\delta}$ crystals. Circles: $M = \text{Zn}$; triangles $M = \text{Fe}$, squares: $M = \text{Ni}$.

the extrapolated onset of the diamagnetic signal in Fig. 3. The initial slope $dT_c/dx \approx -5$ K/at. % is identical within the experimental scattering of the data points for the Fe- and Ni-doped crystals, and the two data points for the Zn-doped crystals fall on the same curve. The initial slope dT_c/dx is in good agreement with the value given for $\text{Bi}(2:2:1:2)$ single crystals doped with Co in Ref. 18. For polycrystalline $\text{Bi}(2:2:1:2)$ dT_c/dx given in the literature is different, namely -2.5 K/at. % for Ni and -7 K/at. % for Fe,²² but we would attribute this to the uncertainty in the determination of the true dopant concentration within the grains of the polycrystalline material. We conclude that the shift of the transition temperature with doping in the $\text{Bi}(2:2:1:2)$ phase depends on the concentration of the dopant only, and neither on the values of the spin, nor on the valency, which is 3+ for Co and Fe,²¹ and 2+ for Ni and Zn. In this respect, the system closely resembles the system $(\text{La}_{1-x}\text{Sr}_x)_2\text{CuO}_4$.^{4,5}

In Fig. 5 we show the result of our $\rho_{ab}(T)$ measurements. One finds that the substitutional atoms strongly affect the resistivity, but in a different manner for Ni and

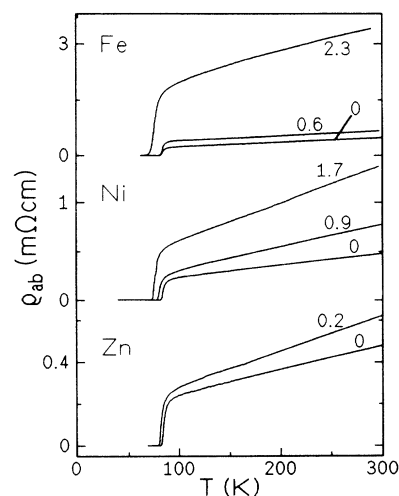


FIG. 5. Electrical resistivity versus temperature for $\text{Bi}(2:2:1:2)$ single crystals doped with Fe, Ni, and Zn. The numbers in the figure give the dopant concentration in at. % of Cu.

Zn on the one hand and for Fe on the other hand. For Ni and Zn mainly the slope $d\rho/dT$ increases (see Table I), the residual resistivity determined by extrapolating the linear slope changing only little. For the Fe-doped system both the residual resistivity and the slope increase strongly with the Fe concentration.

In a conventional Fermi-liquid picture, this would mean that Ni and Zn impurities contribute mainly a temperature-dependent, inelastic-scattering rate whereas Fe impurities add both a temperature-independent elastic-scattering rate and a temperature-dependent inelastic rate. The elastic-scattering rate could be attributed to scattering on the additional electric charge of Fe^{3+} . A strong change of the inelastic-scattering rate at small doping levels is rather unexpected for static impurities.

In Anderson's model of the linear resistivity,¹ a dopant in the CuO_2 planes is expected to introduce a temperature-independent magnetic-scattering rate. Changes of $d\rho/dT$ could be due to changes in the charge-carrier concentrations or the geometry of the Fermi surface. Because of the low concentration of the doping elements and the insensitivity of the Hall effect even at much higher concentration in Fe-doped $\text{Bi}(2:2:1:2)$,²⁶ we can exclude this possibility. The change of resistivity with doping in the $\text{Bi}(2:2:1:2)$ crystals can be compared with that in Zn-doped crystals of $\text{YBa}_2\text{Cu}_3\text{O}_{7-\delta}$.²⁷ There, the residual resistivity with substitution of Zn^{2+} changes at a similar rate as observed in the $\text{Bi}(2:2:1:2)$ crystals; the change of slope, however, is much stronger in the doped $\text{Bi}(2:2:1:2)$ crystals.

In Fig. 6 we show a set of dc screening curves with the magnetic field parallel to the c axis in the field range up to 300 Oe for the crystals containing Fe. With increasing Fe concentration, the screening curves for constant field shift towards lower temperatures. For a crystal with 4.6 at. % Fe even a field of 33 Oe cannot be screened completely at 4 K, indicating that the critical current of this sample is very low.

From the reversible part of the magnetization in Fig. 6, which corresponds to the first linear part of the screening curves, it is possible to extract the Ginzburg-Landau penetration depth in the (ab) plane λ_{ab} . The Abrikosov-London result for $M(H)$ in the magnetic field range $H_{c1} \ll H \ll H_{c2}$ reads²⁸

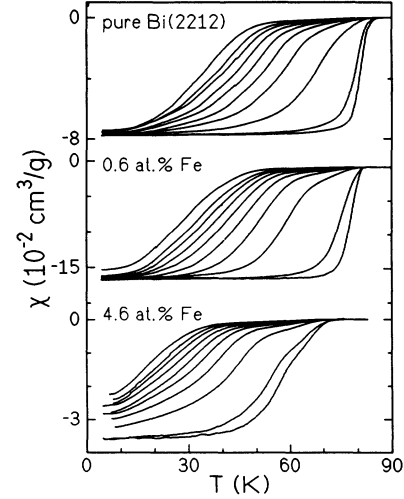


FIG. 6. Magnetic susceptibility versus temperature for $\text{Bi}(2:2:1:2)$ crystals with doping of Fe in a field perpendicular to the (ab) plane at $H = 2, 5, 33, 66, 99, 132, 165, 198, 231, 297$ Oe (from right to left).

$$-M = \frac{\Phi_0}{32\pi^2\lambda_{ab}^2(T)} \ln \left[\frac{\eta H_{c2}(T)}{H} \right], \quad (1)$$

with Φ_0 being the flux quantum, H_{c2} the upper critical field, and η a constant of order unity. With the Ginzburg-Landau type of temperature dependence $\lambda(T) = \lambda_0/(1 - T/T_c)^{1/2}$ we get

$$-\frac{dM}{dT} = -\frac{\Phi_0}{32\pi^2\lambda_0^2 T_c} \ln \left[\frac{\eta H_{c2}(T)}{H} \right] + \frac{\Phi_0(1 - T/T_c)}{32\pi^2\lambda_0^2} \frac{1}{H_{c2}(T)} \frac{dH_{c2}(T)}{dT}. \quad (2)$$

An estimation using $H_{c2}(T)$ derived below shows that the second term is negligible in the field and temperature range of interest here; thus we can derive λ_0 from the first term by taking the logarithmic derivative of $dM(H)/dT$.

In Fig. 7 we show the internal susceptibility $\chi_i = \chi_{\text{ext}}/(1 - N\chi_{\text{ext}})$ corrected for the demagnetizing

TABLE I. Summary of the data derived from the resistivity and the reversible susceptibility. The columns give (from left to right) the concentration, the residual resistivity, the slope of the resistivity, the London penetration depth, the coherence length, and the Ginzburg-Landau parameter.

x	ρ_{res} ($\mu\Omega \text{ cm}$)	$d\rho/dT$ ($\mu\Omega \text{ cm/K}$)	λ_L (\AA)	$\xi_{ab}(0)$ (\AA)	κ
0 at % Fe	83 (± 13)	1.4 (± 0.2)	2200 (± 110)	16.9 (± 0.9)	130 (± 13)
0.6 at % Fe	260 (± 20)	1.9 (± 0.2)	2640 (± 100)	22.0 (± 1.5)	120 (± 20)
1.8 at % Fe			2670 (± 100)		
2.3 at % Fe	1500 (± 100)	6.9 (± 0.7)			
4.6 at % Fe			3460 (± 200)		
0.9 at % Ni	97 (± 10)	2.2 (± 0.2)	2640 (± 150)	12.1 (± 0.5)	218 (± 20)
1.7 at % Ni	180 (± 12)	3.9 (± 0.3)	2590 (± 100)	11.8 (± 0.5)	219 (± 20)
0.2 at % Zn	110 (± 10)	1.7 (± 0.2)	2720 (± 150)	12.9 (± 0.5)	211 (± 20)

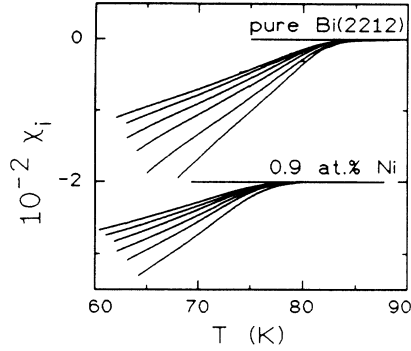


FIG. 7. Reversible internal susceptibility versus temperature at $H = 297, 231, 198, 165, 132, 99$ Oe (from top to bottom curve) for a pure Bi(2:2:1:2) crystal and a crystal with 0.9 at. % Ni (note the offset of the y axis by two units in the lower curves).

field. The mean slope of these curves multiplied by the mean internal field H_i is given in Fig. 8. From the slopes in Fig. 8 and formula (2) we get the London penetration depth given in the fourth column of Table I. The numerical value of $\lambda_L = 2200$ Å for the pure Bi(2:2:1:2) phase is in good agreement with results from the literature.^{29,30} We find that the penetration depth increases definitely upon doping by about 20% for all crystals at low doping concentrations.

For a BCS superconductor, a reduced mean free electron path l changes the penetration depth λ_0 and the coherence length ξ_0 . In the London limit $\xi_0 \ll \lambda_0$, the Pippard coherence length should decrease via

$$\xi = \frac{\xi_0}{1 + \xi_0/l}, \quad (3)$$

and the penetration depth should increase by

$$\lambda = \lambda_0 \sqrt{1 + \xi_0/l}. \quad (4)$$

Although we have observed an increase of λ qualitatively consistent with formula (4), the quantitative agreement is

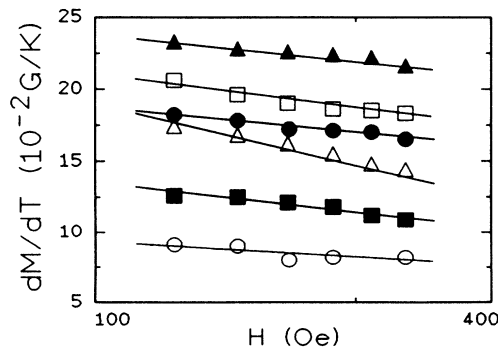


FIG. 8. Numerically determined thermal derivative of the magnetization versus internal magnetic field for a pure Bi(2:2:1:2) single crystal (empty triangles) and a crystal with 0.6 at. % Ni (filled squares), 1.7 at. % Ni (empty squares), 0.6 at. % Fe (filled circles), 4.5 at. % Fe (empty circles), and 0.2 at. % Zn (filled triangles).

bad, when we calculate the relative change of the elastic mean free path l from the relative change of the resistivity given in Table I.

In Fig. 9 we show measurements of the magnetoresistance in a perpendicular magnetic field for the doped crystals in comparison with a pure Bi(2:2:1:2) crystal. From these measurements we tried to derive the upper critical field using the scaling concept worked out by Ullah and Dorsey.³¹ The scaling analysis, however, was not successful, probably because in the magnetic-field range for the measurements in Fig. 9 we are not in the high-field limit required by the theory.

We thus used an empirical procedure to obtain the relative shift of the upper critical field close to T_c with doping by taking 80% of the ρ_n value as a relative measure of the shift of $H_{c2}(T)$. A comparison with the more accurate scaling analysis for the determination of $H_{c2}(T)$ in Ref. 32 indicates that this procedure gives approximate values for $H_{c2}(T)$. We find in Fig. 10 that for the crystals with doping of Ni and Zn the slope of $H_{c2}(T)$ increases definitely compared to the pure Bi(2:2:1:2) crystal, whereas it definitely decreases in the crystal containing Fe. From the dirty-limit formulas $H_{c2}^c(0) = -0.69 T_c (dH_{c2}/dT)_{T_c}$ (Ref. 33) and $H_{c2}^c(0) = \Phi_0 / 2\pi \xi_{ab}^2(0)$ we have derived the correlation lengths given in Table I.

The decrease of $\xi_{ab}(0)$ observed for the crystals containing Ni and Zn is qualitatively consistent with a shortening of the mean free path and the classical formula (3). The Fe-doped crystal, however, falls completely out of the systematics. We have no straightforward explanation for this behavior but we suppose that possibly a slightly inhomogeneous distribution of Fe might cause an additional broadening of the transition in a magnetic field, and thus the intrinsic correlation length cannot be determined from the magnetoresistance measurements.

We next come to the discussion of the irreversible magnetic behavior of the Bi(2:2:1:2) crystals and its change upon doping. An example of magnetic-hysteresis loops of the crystals containing a small amount of Fe impurities at

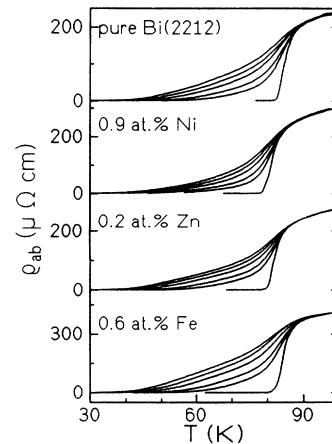


FIG. 9. Resistivity versus temperature in an applied perpendicular magnetic field of $H = 0, 5, 10, 20, 30, 40$ kOe (from right to left) for a pure and for the doped Bi(2:2:1:2) crystals.

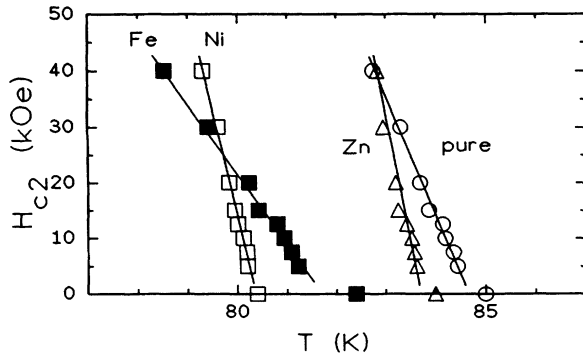


FIG. 10. Upper critical magnetic field versus temperature for a pure Bi(2:2:1:2) single crystal (circles) and crystals doped with 0.9 at. % Ni (empty squares), 0.6 at. % Fe (filled squares), 0.2 at. % Zn (triangles).

different temperatures is shown in Fig. 11. From the irreversible magnetization ΔM between the field-up and field-down branches of the hysteresis loops, the critical current density j_c can be calculated using the standard Bean's model result for the critical state

$$j_c = \frac{20\Delta M}{a(1-a/3b)} \quad (a < b) \quad (5)$$

(cgs units, a and b denote the dimensions of the rectangular crystal perpendicular to the magnetic field parallel to the c axis).^{34,35} We found that $j_c(T)$ has a well-defined value which deviates by less than 20% among different crystals with the same impurity concentration.

In Fig. 12 we compare the critical current $j_c(T)$ at zero field for the doped single crystals at low doping concentration and the pure crystal. One observes that even this low doping concentration deteriorates the critical current definitely by about a factor of 2 at low temperatures. In Fig. 13 we show the critical current for crystals with different Fe concentrations. The absolute value of the critical current decreases strongly with increasing Fe concentrations and is below the experimental limit for temperatures above 40 K in the sample with 4.6 at. % Fe.

The microscopic pinning mechanism in high- T_c com-

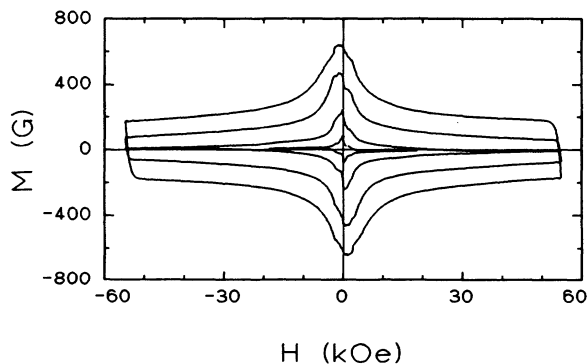


FIG. 11. Magnetic hysteresis loops for a Bi(2:2:1:2) single crystal doped with 0.6 at. % Fe at $T = 4$ (outer curve), 10, 15, and 25 K (inner curve).

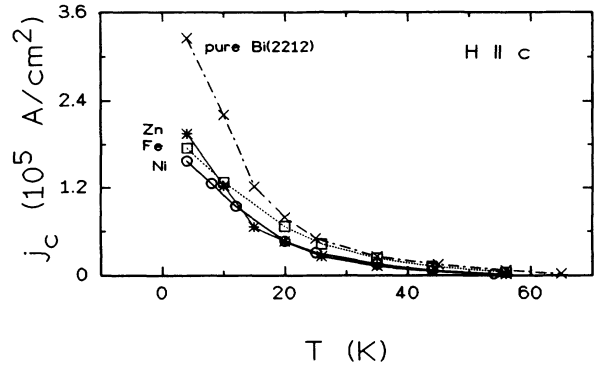


FIG. 12. Critical current density versus temperature at zero magnetic field. Pure Bi(2:2:1:2) (crosses), 0.6 at. % Fe (squares), 0.9 at. % Ni (circles), and 0.2 at. % Zn (stars).

pounds is not well known up to now, but for Bi(2:2:1:2) single crystals point defects, e.g., oxygen vacancies in the CuO_2 planes, have been discussed as the dominant source of pinning centers for the two-dimensional pancake vortices.³⁶ For a pancake vortex, the pinning energy at a pinning center with diameter larger than the core radius is given by

$$U_p = \frac{H_c^2}{8\pi} \pi \xi_{ab}^2 \xi_c \quad (6)$$

Since we have shown above that the correlation length ξ_{ab} decreases at low doping concentration of Ni and Zn the pinning energy and the pinning force should decrease, if one assumes that the pinning mechanism remains essentially unchanged upon doping. This is in good agreement with the observations. Concerning the Fe-doped crystals, the fact that the critical current decreases in a similar way as observed in the Ni- and Zn-doped crystals indicates that probably the value given for the correlation length in Table I is not realistic.

Since we find that the pinning forces are definitely decreasing with doping, we can conclude that the impurities in the CuO_2 planes themselves are not effective as pinning centers. A corresponding additional pinning force at the point defects in the CuO_2 planes could be expected, if one

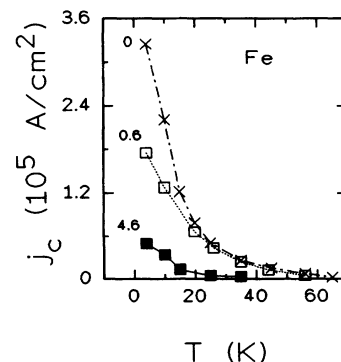


FIG. 13. Critical current density versus temperature at zero magnetic field for Fe-doped Bi(2:2:1:2) single crystals.

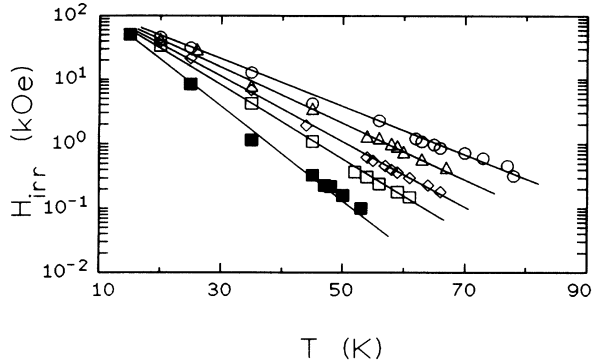


FIG. 14. Irreversibility lines of the single crystals versus temperature. Pure Bi(2:2:1:2) (circles), 0.6 at. % Fe (triangles), 0.9 at. % Ni (diamonds), 0.2 at. % Zn (empty squares), 4.6 at. % Fe (filled squares).

assumes that the superconducting order parameter is suppressed at the doping ions in the CuO_2 planes locally and that point defects can act as effective pinning centers.

From the hysteresis measurements we got the irreversibility lines in the H - T plane by taking the temperature and the field where the irreversibility vanishes (defined as $j_c \leq 20 \text{ A/cm}^2$). The irreversibility lines are plotted in Fig. 14. The low-field values from the SQUID magnetization measurements (Fig. 6) have also been included. Here the irreversibility line is defined by the first deviation of the zero-field- and field-cooled magnetization (not shown in the figure). The irreversibility line $H_{\text{irr}}(T)$ shifts towards lower magnetic field with doping and depends exponentially on temperature. When interpreting $H_{\text{irr}}(T)$ as a thermal depinning line,³⁷ the origin of this shift is the same as discussed in connection with critical current above, namely a reduction of the pinning forces.

Alternatively, adopting the interpretation of the irreversibility line at high fields as a melting transition T_M^{2D} of an essentially two-dimensional vortex lattice,³⁸ one expects

$$T_M^{2D} \approx 0.01 \frac{\Phi_0^2 d}{16\pi^2 \lambda_{ab}^2}, \quad (7)$$

with d being the distance between the CuO_2 planes. In this model, too, the irreversibility line is expected to shift towards lower temperatures, since the London penetration depth increases upon doping.

IV. SUMMARY AND CONCLUSION

We were successful in growing single crystals of the Bi(2:2:1:2) high-temperature superconductor with small amounts of Fe, Ni, and Zn in the Cu position. Analysis of the in-plane resistivity ρ_{ab} revealed an unusually strong influence of the dopant. We find that the residual resistivity ρ_{res} increases strongly with the concentration of Fe^{3+} ions, whereas with Zn^{2+} and Ni^{2+} doping there is only a slight increase of ρ_{res} . This indicates that the additional charge of the 3+ ion introduces a very effective elastic-scattering cross section.

The inelastic-scattering rate which causes the slope

$d\rho/dT$ is found to increase strongly for both 2+ and 3+ dopants. At very low doping concentrations this is rather unexpected in a conventional Fermi-liquid picture, if, for example, phonon scattering contributes the dominant inelastic-scattering rate. If, however, one accepts the idea that an inelastic magnetic-scattering process is dominant in the high- T_c superconductors,¹ this might be interpreted as a change of the magnetic fluctuations by the point defects in the CuO_2 planes.

We found clear evidence that at low doping concentrations already the London penetration depth λ and the correlation length ξ change with decrease of the mean free path, in qualitative agreement with the classical electrodynamic theory of a BCS superconductor. The Ginzburg-Landau parameter κ is found to increase strongly upon doping (see Table I). The decrease of the correlation length with doping gives a consistent explanation for the decrease of the pinning forces and the irreversibility lines.

At higher doping levels above 2 at. % substitution the impurities can no longer be regarded as independent. A clear experimental indication of this is that in Mössbauer experiments on Fe-doped Bi(2:2:1:2), a magnetic order at low temperatures has been observed at this low concentration.³⁹ This might partly be due to a clustering of the Fe ions and a change of the microstructure around the Fe atoms,⁴⁰ but we believe that the magnetic order observed far below the percolation limit of Fe in the CuO_2 planes is an indication that the impurities interact via a change of the local Cu magnetism. This would mean that a point defect in the CuO_2 plane causes a much larger magnetic-impurity center with a rather large interaction radius.

The macroscopic magnetic properties observed at higher doping concentrations of Fe support this picture. The samples are characterized by a low screening current, a very broad transition, and a very low magnetic penetration field. All these ingredients indicate a microscopically inhomogeneous superconducting state.

Coming back to the question of which mechanism is responsible for the suppression of T_c at low doping levels, i.e., for the initial slope dT_c/dx , we can draw some conclusions from our present measurements in comparison with literature data on other systems. In the Fe-, Ni-, and Zn-doped Bi(2:2:1:2) single crystals, dT_c/dx has the same value of -5 K/at. \% , in good agreement with the results on Co-doped Bi(2:2:1:2) crystals from the literature.¹⁸ Thus the Bi(2:2:1:2) single crystals exhibit the same behavior as $(\text{La}_{1-x}\text{Sr}_x)_2\text{CuO}_4$ with doping.^{4,3} In the previously published data on polycrystalline material this was not clear.²⁰⁻²²

This gives additional evidence for the conclusion that paramagnetic pair-breaking scattering on the impurity spin is ineffective in p -type high- T_c superconductors. The most probable reason for this fact is a very small exchange integral J_{pd} between the p -type charge carriers and the d -orbitals of the impurity. This is evident, for example, from the observation that in the antiferromagnetic state of $\text{YBa}_2\text{Cu}_3\text{O}_6$ doped by Fe and Ni the magnetic moments of Fe and Ni are paramagnetic down to the lowest temperatures.⁹

By comparing systematic trends within the different

classes of p -type high- T_c superconductors, one can draw some conclusions about the question whether disorder in a two-dimensional electron system or pair-breaking scattering is the dominant process for suppressing T_c . The $\text{Bi}(2:2:1:2)$ phase under study here has the strongest two-dimensional character within the family of high- T_c superconductors; $\text{YBa}_2\text{Cu}_3\text{O}_{7-\delta}$ and $(\text{La}_{1-x}\text{Sr}_x)_2\text{CuO}_4$ are much less anisotropic. Comparing the initial slope $dT_c/dx = -5$ K/at. % for $\text{Bi}(2:2:1:2)$, about -10 K/at. % for $(\text{La}_{1-x}\text{Sr}_x)_2\text{CuO}_4$, and -10 K/at. % for Zn substitution in $\text{YBa}_2\text{Cu}_3\text{O}_{7-\delta}$, one finds no quantitative correlation between the two-dimensional character and dT_c/dx . Furthermore, the mean free path of the electrons in $\text{Bi}(2:2:1:2)$ is far more reduced by doping with Fe and Co than by doping with Ni, but nevertheless the suppression of T_c is identical. Thus the disorder induced by the doping does not seem to be the essential parameter determining the initial slope dT_c/dx .

We conclude that a pair-breaking scattering process induced by the dopants is responsible for the initial suppression of T_c . As stated in the Introduction, the pair-breaking process could be nonmagnetic elastic scattering, if the superconducting order parameter has d symmetry. However, we would not argue in favor of this process, since the total scattering rates of the Fe-doped and the Ni-doped $\text{Bi}(2:2:1:2)$ crystals are very different but dT_c/dx is identical. We think the most probable pair-breaking scattering process is a scattering on paramagnetic, local Cu spins induced close to the doping elements.

ACKNOWLEDGMENTS

The authors thank the DFG for financial support of this work.

- ¹P. W. Anderson, Phys. Rev. Lett. **67**, 2092 (1991).
- ²A. M. Finkelstein, V. E. Kateev, E. F. Kutovskii, and G. B. Teitelbaum, Physica C **168**, 370 (1990).
- ³M. Z. Cieplak, G. Xiao, A. Bakhshai, and L. Z. Chien, Phys. Rev. B **39**, 4222 (1989).
- ⁴J. M. Tarascon, L. H. Greene, P. Barboux, W. R. McKinnon, G. W. Hull, T. P. Orlando, K. A. Delin, S. Foner, and E. J. McNiff, Jr., Phys. Rev. B **36**, 8393 (1987).
- ⁵G. Xiao, A. Bakhshai, M. Z. Cieplak, and L. Z. Chien, Phys. Rev. B **39**, 315 (1989).
- ⁶J. M. Tarascon, E. Wang, S. Kivelson, B. G. Bagley, G. W. Hull, and R. Ramesh, Phys. Rev. B **42**, 218 (1990).
- ⁷S. Yamagata, K. Adachi, M. Onoda, H. Fujishita, M. Sera, Y. Andoama, and M. Sato, Solid State Commun. **74**, 177 (1990).
- ⁸J. Clayhold, N. P. Ong, P. H. Har, and C. W. Chu, Phys. Rev. B **38**, 7016 (1988).
- ⁹K. Westerholt, H. J. Wüller, H. Bach, and P. Stauche, Phys. Rev. B **39**, 11 680 (1989).
- ¹⁰R. Sonntag, D. Hohlwein, A. Hoser, W. Prandl, W. Schäfer, R. Kiemel, S. Kemmler-Sack, S. Lösch, M. Schlichenmaier, and A. W. Hewat, Physica C **159**, 141 (1989).
- ¹¹J. Clayhold, S. Hagen, Z. Z. Wang, N. P. Ong, J. M. Tarascon, and P. Barboux, Phys. Rev. B **39**, 777 (1989).
- ¹²R. S. Howland, T. H. Geballe, S. S. Laderman, A. Fischer-Colbrie, M. Scott, J. M. Tarascon, and P. Barboux, Phys. Rev. B **39**, 9017 (1989).
- ¹³F. Bridges, J. B. Boyce, T. Claeson, T. H. Geballe, and J. M. Tarascon, Phys. Rev. B **42**, 2137 (1990).
- ¹⁴H. Fukuyama, Physica B+C **126B**, 306 (1984).
- ¹⁵W. Brenig, M. A. Paalanen, A. F. Hebard, and P. Wölffe, Phys. Rev. B **33**, 1691 (1986).
- ¹⁶G. Roth, P. Adelman, R. Ahrens, B. Blank, H. Bürkle, F. Gompf, G. Heger, M. Hervieu, M. Nindel, B. Obst, J. Panetier, B. Raveau, B. Renker, H. Rietschel, B. Rudolf, and H. Wühl, Physica C **162-164**, 518 (1989).
- ¹⁷E. Seider, M. Bauer, L. Genzel, P. Wyder, A. Jansen, and C. Richter, Solid State Commun. **72**, 85 (1989).
- ¹⁸M. Boekholt, Th. Bollmeniner, L. Buschmann, M. Fleuster, and G. Güntherodt, Physica C **198**, 33 (1992).
- ¹⁹J. F. Foulkes and B. L. Gyorffy, Phys. Rev. B **15**, 1395 (1977).
- ²⁰A. Maeda, T. Tabe, S. Takebayashi, M. Hase, and K. Uchinokura, Phys. Rev. B **41**, 4112 (1990).
- ²¹P. Sumana Prabhu, M. S. Ramachandra Rao, and G. U. Subba Rao, Physica C **211**, 279 (1993).
- ²²B. Lönnberg, T. Lunström, and P. Norling, Physica C **191**, 147 (1992).
- ²³O. Bonfigt, H. Somnitz, K. Westerholt, and H. Bach, J. Cryst. Growth **128**, 725 (1993).
- ²⁴S. Horiuchi, H. Maeda, Y. Tanaka, and Y. Matsui, Jpn. J. Appl. Phys. **27**, L1172 (1988).
- ²⁵R. Kubiak, K. Westerholt, and H. Bach, Physica C **166**, 523 (1990).
- ²⁶K. Uchinokura, T. Yabe, S. Takebayashi, M. Hase, and A. Maeda, Physica C **162-164**, 981 (1989).
- ²⁷T. R. Chien, Z. Z. Wanf, and N. P. Ong, Phys. Rev. Lett. **67**, 2088 (1991).
- ²⁸P. G. de Gennes, *Superconductivity of Metals and Alloys* (Benjamin, New York, 1966).
- ²⁹P. H. Kes, C. J. van der Beek, M. P. Maley, M. E. McHenry, D. A. Huse, M. J. V. Menken, and A. A. Menovsky, Phys. Rev. Lett. **67**, 2383 (1991).
- ³⁰D. R. Harshmann, E. H. Brandt, A. T. Fiory, M. Inui, D. B. Mitzi, L. F. Schneemeyer, and J. V. Waszczak, Phys. Rev. B **47**, 2905 (1993).
- ³¹S. Ullah and A. T. Dorsey, Phys. Rev. B **44**, 262 (1991).
- ³²M. D. Lan, J. Z. Liu, Y. X. Jia, Lu Zhang, Y. Nagata, P. Kalvins, and R. N. Shelton, Phys. Rev. B **47**, 457 (1993).
- ³³N. R. Wethamer, E. Helfand, and P. C. Hohenberg, Phys. Rev. **147**, 295 (1966).
- ³⁴C. P. Bean, Phys. Rev. Lett. **8**, 250 (1962).
- ³⁵E. M. Giorgy, R. B. van Dover, K. A. Jackson, L. F. Schneemeyer, and J. V. Waszczak, Appl. Phys. Lett. **55**, 283 (1989).
- ³⁶C. J. van der Beek, P. H. Kes, M. P. Maley, M. P. V. Menken, and A. A. Menovsky, Physica C **195**, 307 (1992).
- ³⁷E. H. Brandt, Physica C **195**, 1 (1992).
- ³⁸D. S. Fisher, M. P. A. Fisher, and D. A. Huse, Phys. Rev. B **43**, 130 (1991).
- ³⁹C. Saragovi, C. Fainstein, P. Etchegoin, and S. Duhalde, Physica C **168**, 493 (1990).
- ⁴⁰T. Krekels, G. van Tendeloo, D. Broddin, S. Amelnickx, L. Tanner, M. Mehbod, E. Vanlathem, and R. Deltour, Physica C **173**, 361 (1991).